

The anti-tumor drug bleomycin preferentially cleaves at the transcription start sites of actively transcribed genes in human cells

Vincent Murray · Jon K. Chen · Anne M. Galea

Received: 2 June 2013 / Revised: 6 August 2013 / Accepted: 12 August 2013 / Published online: 28 August 2013
© Springer Basel 2013

Abstract The genome-wide pattern of DNA cleavage at transcription start sites (TSSs) for the anti-tumor drug bleomycin was examined in human HeLa cells using next-generation DNA sequencing. It was found that actively transcribed genes were preferentially cleaved compared with non-transcribed genes. The 143,600 identified human TSSs were split into non-transcribed genes (82,596) and transcribed genes (61,004) for HeLa cells. These transcribed genes were further split into quintiles of 12,201 genes comprising the top 20, 20–40, 40–60, 60–80, and 80–100 % of expressed genes. The bleomycin cleavage pattern at highly transcribed gene TSSs was greatly enhanced compared with purified DNA and non-transcribed gene TSSs. The top 20 and 20–40 % quintiles had a very similar enhanced cleavage pattern, the 40–60 % quintile was intermediate, while the 60–80 and 80–100 % quintiles were close to the non-transcribed and purified DNA profiles. The pattern of bleomycin enhanced cleavage had peaks that were approximately 200 bp apart, and this indicated that bleomycin was identifying the presence of phased nucleosomes at TSSs. Hence bleomycin can be utilized to detect chromatin structures that are present at actively transcribed genes. In this study, for the first time, the pattern of DNA damage by a clinically utilized cancer chemotherapeutic agent was performed on a human genome-wide scale at the nucleotide level.

Keywords Anti-tumor agent · Bleomycin · Chromatin · DNA damage · Next-generation sequencing

Abbreviations

TSS Transcription start site
MNase Micrococcal nuclease

Introduction

The glycopeptide antibiotic bleomycin is used as a cancer chemotherapeutic agent to treat squamous cell carcinoma, Hodgkin's lymphoma, and testicular cancer [1–3]. Its mechanism of action is thought to involve DNA damage and DNA cleavage [4]. Both double-strand and single-strand breaks are formed by bleomycin although double-strand breaks are thought to be most important for the anti-tumor activity of bleomycin [5].

The reaction of bleomycin with DNA requires a divalent cation, usually Fe^{2+} . The reaction mechanism for the damage and cleavage of DNA involves the abstraction of a hydrogen atom from the C4' of the deoxyribose sugar in DNA. The resulting free radical then reacts with O_2 and ultimately leads to breakage of the DNA phosphodiester backbone with production of 3'-phosphoglycolate and 5'-phosphate ends and a pyrimidine propenal [6–11].

Previous bleomycin DNA sequence specificity studies with purified plasmid DNA sequences have indicated that the dinucleotides 5'-GT and 5'-GC are preferentially cleaved [12–16]. The DNA sequence specificity has also been determined in human cells at centromeric alphoid DNA sequences [17], telomeric DNA sequences [18], globin [19–22], and retinoblastoma genes [23]; and the DNA sequence specificity was again found to be mainly at the dinucleotides 5'-GC and GT in human cells. For globin and

Electronic supplementary material The online version of this article (doi:10.1007/s00018-013-1456-4) contains supplementary material, which is available to authorized users.

V. Murray (✉) · J. K. Chen · A. M. Galea
School of Biotechnology and Biomolecular Sciences, University of New South Wales, Sydney, NSW 2052, Australia
e-mail: v.murray@unsw.edu.au

retinoblastoma DNA sequences, the bleomycin was able to footprint transcription factors and positioned nucleosomes in human cells. Bleomycin is known to cleave in the linker region of nucleosomes [17, 24, 25] and hence bleomycin is a useful agent to probe chromatin structure in human cells.

Next-generation sequencing techniques have been employed to examine several areas of molecular biology [26–28]. The Illumina Hi-Seq 2000 can generate more than 200 million short sequences in a single run. DNase I hypersensitive sites have been mapped at high resolution [29, 30] and shown to be associated with promoters, enhancers, insulators and locus control regions [31]. Next-generation sequencing has also been useful in demonstrating that these open chromatin regions are associated with post-translational histone modifications. The location of acetylated and non-acetylated histones, as well as methylated histones and positioned nucleosomes, has also been pinpointed with precision [32–39].

In this study we examined the cleavage sites of bleomycin in the entire human genome in human cells. We utilized next-generation sequencing techniques to map the double-strand break sites of bleomycin onto the entire human DNA sequence. This enabled features such as transcription start sites (TSSs) and chromatin structure to be correlated with the sites of bleomycin cleavage. This study represents the first occasion that the DNA damage sites of an anti-tumor agent have been mapped at high resolution for the entire human genome.

Materials and methods

Bleomycin was obtained from Bristol Laboratories (USA). Endonuclease IV was purchased from New England Biolabs. Human HeLa cells were treated with 0.5 mM bleomycin for 30 min at 37 °C in phosphate buffered saline and the DNA was extracted from the cells [17]. In parallel, purified HeLa DNA was treated with 0.33 mM bleomycin [17]. The bleomycin-treated purified DNA and purified bleomycin-treated cellular DNA were treated with the enzyme endonuclease IV to remove 3'-phosphoglycolate termini with its 3'-diesterase activity [40]. The 3'-phosphoglycolate termini are not removed by the "polishing" 3'-5'-exonuclease reaction of DNA polymerase I and hence the endonuclease IV treatment was necessary in order that the bleomycin cleavage site were compatible with the Illumina preparation procedure of 3'-A addition and subsequent ligation of the linker oligonucleotides. The CplusE and #1CplusE cellular samples were treated with endonuclease IV (these two samples are duplicates from independent experiments); the CminE cellular sample was not treated with endonuclease IV; while the DplusE purified DNA sample was treated with endonuclease IV.

After linker addition, the bleomycin-treated DNA samples were electrophoresed and purified on an Agilent Technologies 2100 expert high sensitivity DNA assay system. DNA fragments between 200 and 1,000 bps were purified and subjected to DNA sequencing in an Illumina flow cell.

The resulting DNA sequence reads were mapped onto the hg19 repeat masked human genome sequence with Bowtie [41]. Using Samtools [42], the mapped reads were sorted and unmapped reads were removed. With HTSeq in the Python environment (<http://www-huber.embl.de/users/anders/HTSeq/doc/tss.html#tss>), the bleomycin cleavage sites were mapped onto HeLa cell transcription start sites (TSSs).

The 143,600 HeLa TSSs were obtained from the file "J80-J81_TSSGencv7.gff" obtained from "<http://genome.ucsc.edu/cgi-bin/hgFileUi?db=hg19&g=wgEncodeRikenCage>" as the file "wgEncodeRikenCageHelas3CellPapTssGencV7.gtf.gz".

The 143,600 HeLa TSSs were split into the 82,596 TSSs with zero expression and 61,004 TSSs with some expression level. These 61,004 TSSs were further categorized into five quintiles of differing expression levels, 0–20, 20–40, 40–60, 60–80, and 80–100 %, with the 0–20 % being the highest expressed TSSs and the 80–100 % TSSs being the lowest expressed in HeLa cells. The relative range of expression for the 0–20 % quintile was 1000 to 1.9, for the 20–40 % quintile 1.9 to 0.35, 40–60 %, 0.35 to 0.041, 60–80 %, 0.041 to 0.0062, and 80–100 %, 0.0062 to 0.0018.

Using HTSeq, bleomycin cleavage sites for these six categories of HeLa expression were mapped to within 3,000 bp of the TSS using a sliding window (fragment size) of 10 bp. Using a similar methodology, the bleomycin cleavage sites were also mapped onto the sense and anti-sense strands [34].

The RNA-seq data "J80-DA_20100603_Solexa_HWUSI-EAS566_lane5.txt" was downloaded from "<http://hgdownload-test.cse.ucsc.edu/goldenPath/hg19/encodeDC/wgEncodeRikenCage/>" as the file "wgEncodeRikenCageHelas3CellPapRawDataRep1.fastq.gz".

Results

For all four of the samples, a read length of 51 nucleotides was produced. The CminE sample produced 2.53×10^8 sequences of which 96.7 % mapped to the hg19 human genome;

CplusE produced 2.42×10^8 sequences (96.8 % mapped); DplusE -2.17×10^8 sequences (94.7 % mapped); and #1CplusE -5.79×10^7 sequences (96.8 % mapped).

Preliminary results with 143,600 human TSSs indicated that enhanced cleavage was present for bleomycin at TSSs.

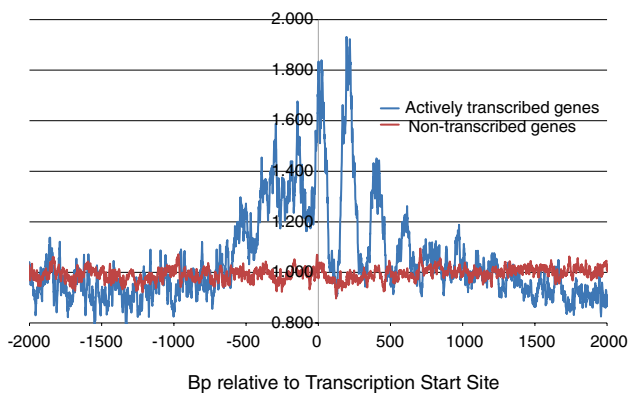


Fig. 1 Bleomycin damage at transcription start sites for actively transcribed genes and non-transcribed genes in human HeLa cells. The actively transcribed genes (*blue*) comprise the combined 0–20 and 20–40 % quintiles and are the 24,402 most highly expressed genes in HeLa cells. The non-transcribed genes (*red*) comprise the 82,596 non-transcribed genes in HeLa cells. The data is from the Cplus and Dplus samples and the y-axis is the ratio of the cellular/purified DNA values at each nucleotide surrounding the TSS (x-axis)

In order to examine the effect of transcriptional activity on the enhanced cleavage, the 143,600 identified human TSSs were split into non-transcribed genes (82,596) and transcribed genes (61,004), which were further sub-divided into five quintiles.

In Fig. 1, the cellular bleomycin cleavage sites were mapped on the combined top 20 and 20–40 % quintiles of genes. In Fig. 1 the values are presented as a ratio of cellular bleomycin DNA cleavage compared with purified DNA at each nucleotide. Hence, any bias due to the varying DNA cleavage specificity of bleomycin was removed. Enhanced cleavage of up to twofold was observed for the top 40 % quintiles compared with the non-transcribed genes. Actively transcribed genes were preferentially cleaved by bleomycin within approximately 700 bp of the TSS.

A further point to notice is that the peaks were approximately 200 bp apart, especially downstream of the TSS. This indicated that phased nucleosomes were present in these regions. There is also an indication that the peaks were multiple in nature that could be caused by overlapping genes that were slightly out of phase.

In Supplementary Figure 1 bleomycin cleavage sites at the TSSs were mapped for the five expressed quintiles as well as the non-expressed genes. The top 20 and 20–40 % quintiles had a similar profile, while the 40–60 % quintile was intermediate. The 60–80 and 80–100 % quintiles were close to the non-expressed gene profile. This was quantified in Fig. 2 where the enhancement above the ratio of 1 was summated between –700 and +700 bp around the TSS. It can be seen in Fig. 2 that as the level of transcription declines, the degree of enhancement is also reduced, especially from the 20–40 % quintile to the 80–100 %

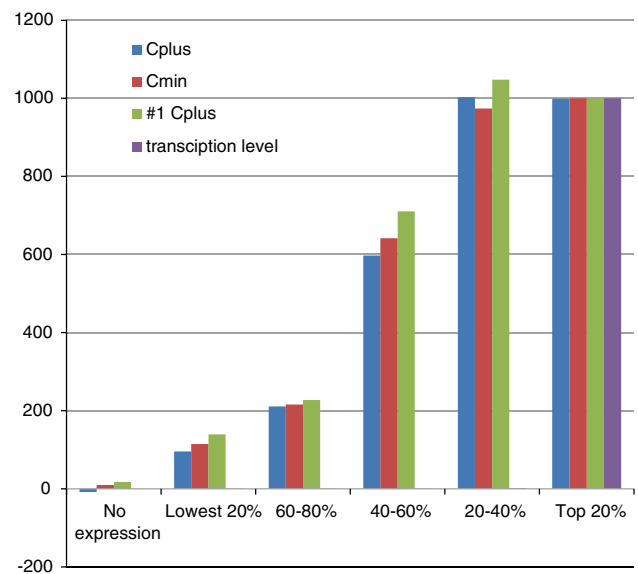


Fig. 2 The relationship between the level of gene expression and enhancement of bleomycin cleavage at the TSSs. The enhancement of the bleomycin cleavage ratio (cellular/purified DNA) between –700 and 700 bp was quantified for each of the five expression quintiles and for the non-transcribed genes. The transcription level for each of the quintiles is also indicated on the column graph (*purple*). The enhancement of the bleomycin cleavage ratio is presented for the Cplus (*blue*), Cmin (*red*), and #1Cplus samples (*green*). The y-axis is the normalized bleomycin enhancement ratio and has been normalized to an arbitrary value of 1,000 for the top 20 % quintile

quintile. However, the level of enhancement is not precisely related to the level of transcription since the top 20 and 20–40 % quintiles had a similar profile but the level of transcription varied by over 1,000-fold within these quintiles (Fig. 2). In Fig. 2, the three different cellular samples all gave a very similar pattern for the five quintiles of gene expression and no expression. These similar patterns from independent experiments gives confidence that the result is reproducible.

The bleomycin cleavage sites were also mapped onto the sense and antisense strands at the TSSs (Fig. 3a). Peaks with spacing of approximately 200 bp were seen for both sense and antisense strands. There was also a slight offset between the two strands. Figure 3b shows data from a study utilizing micrococcal nuclease as the cleaving agent in CD4+ human nuclei [34]. It can be seen that the bleomycin data is very similar to the micrococcal nuclease data for the regions –1,000 to –200 and 0 to 1,000 bp on the sense strand and –1,000 to –100 and 100 to 1,000 bp on the antisense strand. However, between –200 to 0 bp (sense) and –100 to 100 bp (antisense), there were peaks at –120 bp (sense) and 0 bp (antisense) for the bleomycin data but there were no peaks in the same regions for the micrococcal nuclease data (Fig. 3b). Nucleosomes are not thought to be present in these regions at the TSSs [34].

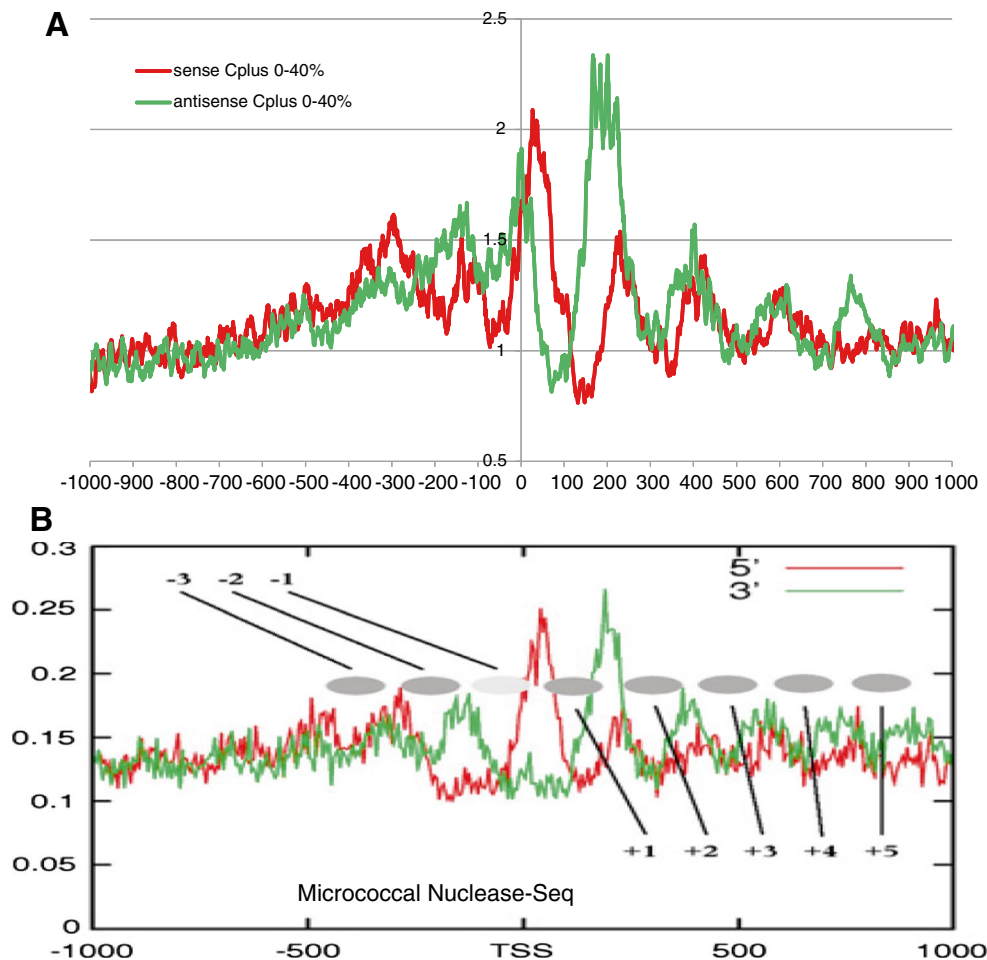


Fig. 3 The bleomycin cleavage ratio for the sense and antisense strands at the TSSs as well as Micrococcal Nuclease-Seq data. **a** The bleomycin cleavage ratio (cellular/purified DNA) for the combined 0–20 and 20–40 % quintiles for the sense (*red*) and antisense (*green*) strands. The data is from the Cplus and Dplus samples and the y-axis

is the ratio of the cellular/purified DNA values at each nucleotide surrounding the TSS (*x*-axis). **b** Comparison data for Micrococcal Nuclease-Seq on the sense (*red*) and antisense (*green*) strands is shown and has been reprinted from Schones et al. [34]. Positioned nucleosomes are indicated

The bleomycin cleavage sites at the TSSs were mapped for the five expressed quintiles and the non-expressed genes for the sense strand (Supplementary Figure 2a) and the antisense strand (Supplementary Figure 2b). The top 20 and 20–40 % quintiles had a similar profile for each strand, while the 40–60 % quintile was again intermediate. The 60–80 and 80–100 % quintiles were close to the non-expressed gene profile.

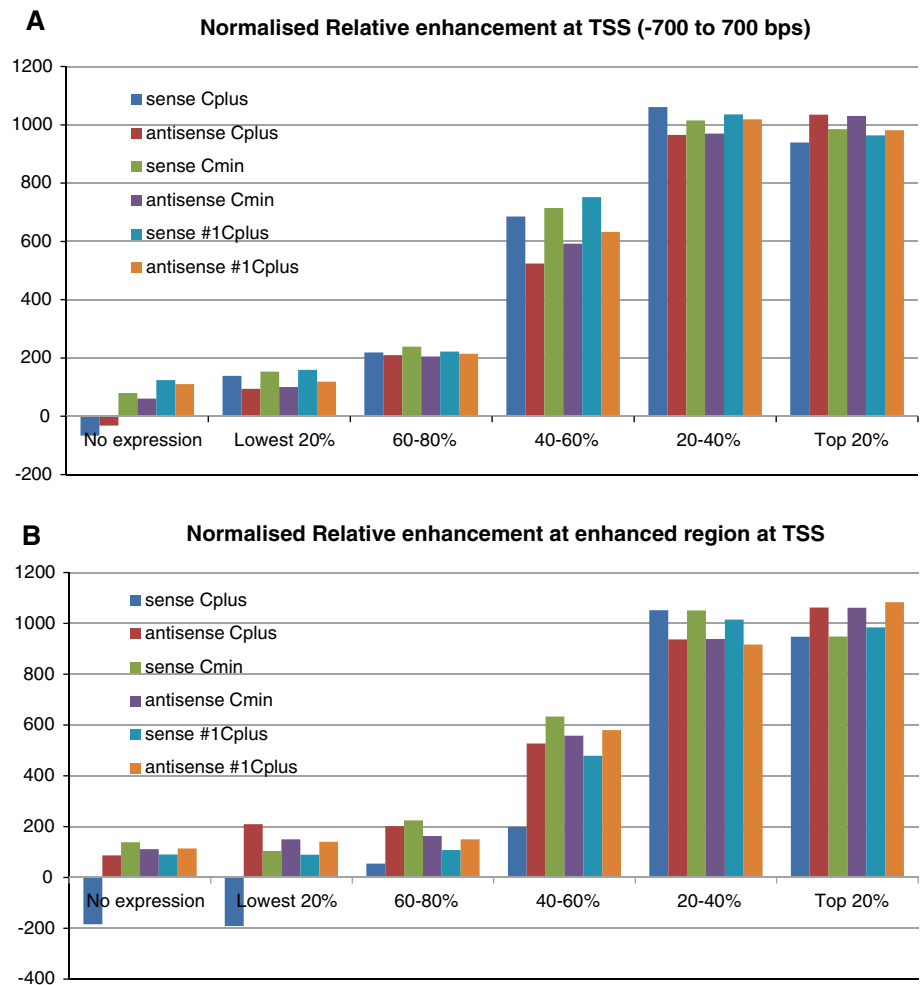
The sense and antisense bleomycin data were quantified for the region from –700 to 700 bp around the TSSs for the sense and antisense strands (Fig. 4a). The profiles for the five quintiles and no expression data showed a decline in enhancement with the decline in the level of gene expression, especially from the 20–40 % quintile to the 80–100 % quintile. This Fig. 4a data was very similar on both strands, for the three different cellular samples, and also compared with the combined strand data in Fig. 2.

The extra enhanced peaks at –120 bp (sense) and 0 bp (antisense) in the bleomycin data compared with the micrococcal nuclease data (see above) were quantified as shown in Fig. 4b. The profile of these peaks with respect to the level of gene expression was very similar to the –700 to 700 bp enhancement in Fig. 4a.

The bleomycin cleavage data for the sense and antisense strands is shown in Supplementary Figure 3 with the location of the positioned nucleosomes superimposed. It can be seen that the nucleosomes are slightly offset, with the sense strand nucleosomes approximately 30 bp to the right of the antisense strand nucleosomes. There is space for a potential nucleosome between approximately –140 and 40 bp.

The protocols and procedures for mapping the bleomycin data to the sense and antisense strands was verified by using RNA-seq data from HeLa cells. As can be seen in Supplementary Figure 4, the HeLa RNA-seq data mapped

Fig. 4 The relationship between the level of gene expression and enhancement of bleomycin cleavage on the sense and antisense strands at the TSSs. The enhancement of the bleomycin cleavage ratio is presented for each of the five expression quintiles and for the non-transcribed genes on the sense and antisense strands with the Cplus, Cmin and #1Cplus samples. The y-axis is the normalized bleomycin enhancement ratio and has been normalized to an arbitrary value of 1,000 for the top 20 % quintile. **a** The enhancement of the bleomycin cleavage ratio (cellular/purified DNA) between -700 and 700 bp relative to the TSS. **b** The enhancement of the bleomycin cleavage ratio (cellular/purified DNA) between -170 and -60 bp on the sense strand and between -90 and 30 bp on the antisense strand



almost entirely to the sense strand as expected and not to the antisense strand.

Discussion

In this study, for the first time, the pattern of DNA cleavage for an anti-tumor drug was determined at high resolution for the entire human genome in human cells. Bleomycin is utilized as a cancer chemotherapeutic agent to treat Hodgkin's lymphoma, squamous cell carcinoma, and testicular cancer [1–3]. Since the mechanism of action of bleomycin is thought to involve DNA damage and DNA cleavage [4], it is very important to determine the position of the bleomycin cleavage sites.

The preferred sites of bleomycin cleavage are at 5'-GT and 5'-GC dinucleotides [12–16]. In order to allow for varying bleomycin cleavage efficiencies at different nucleotide sequences, a ratio of cellular to purified DNA bleomycin cleavage was calculated at each nucleotide. This enabled

any bias due to the DNA sequence specificity of bleomycin cleavage to be removed.

The main outcome of this study was that bleomycin preferentially cleaved at the transcription start sites (TSSs) of actively transcribed genes compared with non-transcribed genes. Bleomycin is a relatively large molecule (molecular weight approximately 1,500 Daltons) and would have difficulty in accessing the closed chromatin structures of non-transcribed genes [19, 25]. This indicated that genes with an open configuration gave bleomycin easy access to DNA compared with closed structures where DNA is protected by histones and other proteins in chromatin [17]. It has previously been shown that bleomycin preferentially cleaved actively expressed ovalbumin and globin genes but no preferential cleavage occurred when these genes were not being expressed [43].

The enhanced bleomycin cleavage at TSSs correlated with the level of transcriptional activity. There was a gradual reduction in the level of enhanced bleomycin cleavage from the 20–40 % quintile to the 80–100 % quintile;

however, the enhanced bleomycin cleavage was similar for the 0–20 % and 20–40 % quintiles (see below).

This information could be used to enhance the cancer chemotherapeutic activity of bleomycin. Targeting of these actively transcribed genes in conjunction with bleomycin treatment could enhance the cancer chemotherapeutic efficacy of bleomycin by the down-regulation of these highly expressed genes [44, 45].

It should be noted that the concentrations used in this study are higher than those in a clinical setting. Several studies have shown that the DNA sequence specificity of bleomycin is similar over a range of concentrations in cellular and purified DNA [17, 46, 47]. However, it has also been demonstrated that at very low bleomycin concentrations with small hairpin oligonucleotide sequences, bleomycin has a different sequence specificity [48–50].

The pattern of DNA cleavage had a peak-to-peak distance of approximately 200 bp. This indicated that positioned nucleosomes exist at actively transcribed genes as found by others in yeast [32, 33] and human cells [34]. This correlated with the known ability of bleomycin to cleave in the linker region of nucleosomes [17, 24, 25].

The detection of similar enhanced bleomycin cleavage patterns in the top 20 and 20–40 % quintiles suggests that a particular chromatin structure is being recognized by bleomycin. The degree of transcription varied by over a 1,000-fold within these two quintile groups. Hence, this chromatin structure, detected by bleomycin, does not predict the level of transcription but indicates a potential for high-level transcription. Further factors, e.g., the recruitment of transcription factors, would be expected to be required for high-level transcription to be achieved.

The peaks at 0 bp on the sense strand and –120 bp on the antisense strand were not found in the micrococcal nuclease experiments (MNase-seq) [34]. There are several explanations for these differences. First, in the micrococcal nuclease experiments the nucleosomal linker DNA is trimmed back to the nucleosome core and hence any free DNA that is not present in the nucleosome core is digested away. However, in the bleomycin experiments, the DNA is not trimmed back to the core and any free (linker) DNA will be included in the analysis. Another difference is that CD4+ cells were used for the MNase-seq experiments while it was HeLa cells for the bleomycin experiments.

Second, the bleomycin experiments could be detecting nucleosomes. The peaks at 0 bp on the sense strand and –120 bp on the antisense strand are approximately 200 bp from the neighboring peaks and that is characteristic of the presence of a nucleosome core. However, other experiments with anti-histone antibodies have indicated that a nucleosome is not present in this part of the gene [34, 51]. The bleomycin experiments may be revealing the transient presence of a nucleosome [52, 53].

Third, the bleomycin experiments may be detecting a particular structural element at TSSs. Since the bleomycin cleavage is enhanced at this region, it could have been caused by a structural distortion in the DNA. An unusual structural distortion in the DNA at the TSS could be present as part of the transcriptional initiation complex. Alternatively, a large protein (or complex) could be present on one side of the enhanced region. A strong candidate for a large protein complex would be the RNA polymerase complex, which has similar dimensions to that of a nucleosome and would fit into the DNA region between the peaks. There are several arguments against the presence of the RNA polymerase complex in these regions. RNA polymerase should only be bound to the antisense strand and in our experiments the peak was found on both strands. Also anti-RNA polymerase antibody pull-downs [34] indicate that the RNA polymerase is present at 0 bp at the TSS, i.e., not in the region between the peaks but at the peak.

Fourth, the extra enhanced peaks at –120 bp (sense) and 0 bp (antisense) had a similar profile with respect to the level of gene expression compared with the –700 to 700 bp enhancement (Fig. 4). This indicates that structure at the TSS that is being detected by bleomycin is present to a similar degree at the –120-bp and 0-bp sites as the overall enhancement structure, and is probably part of TSS structure that is poised for transcription.

Conclusions

In conclusion, we have shown for the first time the pattern of bleomycin cleavage for the whole genome in human cells. Bleomycin cleavage was preferentially observed at the TSSs of expressed genes. This study provided insight into the mechanism of action of this anti-tumor drug where actively transcribed genes were preferentially targeted. This information could be utilized to enhance the activity of bleomycin and other anti-tumor drugs.

Acknowledgments This work was supported by the University of New South Wales, Science Faculty Research Grant Scheme. Technical assistance by Shweta Dutta is gratefully acknowledged.

References

1. Umezawa H, Maeda K, Takeuchi T, Okami Y (1966) New antibiotics, bleomycin A and B. *J Antibiot* 19:200–209
2. Stoter G, Kaye SB, de Mulder PH, Levi J, Raghavan D (1994) The importance of bleomycin in combination chemotherapy for good-prognosis germ cell carcinoma. *J Clin Oncol* 12:644–645
3. Einhorn LH (2002) Curing metastatic testicular cancer. *Proc Natl Acad Sci USA* 99:4592–4595
4. Sikic BI (1986) Biochemical and cellular determinants of bleomycin cytotoxicity. *Cancer Surv* 5:81–91

5. Mirabelli CK, Huang CH, Fenwick RG, Croke ST (1985) Quantitative measurement of single- and double-strand breakage of DNA in *Escherichia coli* by the antitumor antibiotics bleomycin and talisomycin. *Antimicrob Agents Chemother* 27:460–467
6. Burger RM, Berkowitz AR, Peisach J, Horwitz SB (1980) Origin of malondialdehyde from DNA degraded by Fe(II) x bleomycin. *J Biol Chem* 255:11832–11838
7. Giloni L, Takeshita M, Johnson F, Iden C, Grollman AP (1981) Bleomycin-induced strand-scission of DNA. Mechanism of deoxyribose cleavage. *J Biol Chem* 256:8608–8615
8. Stubbe J, Kozarich JW, Wu W, Vanderwall DE (1996) Bleomycins: a structural model for specificity, binding, and double strand cleavage. *Acc Chem Res* 29:322–330
9. Burger RM (1998) Cleavage of Nucleic Acids by Bleomycin. *Chem Rev* 98:1153–1170
10. Chen J, Stubbe J (2005) Bleomycins: towards better therapeutics. *Nat Rev Cancer* 5:102–112
11. Yu Z, Schmaltz RM, Bozeman TC, Paul R, Rishel MJ, Tsosie KS, Hecht SM (2013) Selective tumor cell targeting by the disaccharide moiety of bleomycin. *J Am Chem Soc* 135:2883–2886
12. Takeshita M, Grollman AP, Ohtsubo E, Ohtsubo H (1978) Interaction of bleomycin with DNA. *Proc Natl Acad Sci USA* 75:5983–5987
13. Takeshita M, Kappen LS, Grollman AP, Eisenberg M, Goldberg IH (1981) Strand scission of deoxyribonucleic acid by neocarzinostatin, auroiomycin, and bleomycin: studies on base release and nucleotide sequence specificity. *Biochemistry* 20:7599–7606
14. D'Andrea AD, Haseltine WA (1978) Sequence specific cleavage of DNA by the antitumor antibiotics neocarzinostatin and bleomycin. *Proc Natl Acad Sci USA* 75:3608–3612
15. Murray V, Martin RF (1985) Comparison of the sequence specificity of bleomycin cleavage in two slightly different DNA sequences. *Nucleic Acids Res* 13:1467–1481
16. Murray V, Tan L, Matthews J, Martin RF (1988) The sequence specificity of bleomycin damage in three cloned DNA sequences that differ by a small number of base substitutions. *J Biol Chem* 263:12854–12859
17. Murray V, Martin RF (1985) The sequence specificity of bleomycin-induced DNA damage in intact cells. *J Biol Chem* 260:10389–10391
18. Nguyen HTQ, Murray V (2012) The DNA sequence specificity of bleomycin cleavage in telomeric sequences in human cells. *J Biol Inorgan Chem* 17:1209–1215
19. Cairns MJ, Murray V (1996) Influence of chromatin structure on bleomycin-DNA interactions at base pair resolution in the human beta-globin gene cluster. *Biochemistry* 35:8753–8760
20. Kim A, Murray V (2000) A large “footprint” at the boundary of the human beta-globin locus control region hypersensitive site-2. *Int J Biochem Cell Biol* 32:695–702
21. Kim A, Murray V (2001) Chromatin structure at the 3'-boundary of the human beta-globin locus control region hypersensitive site-2. *Int J Biochem Cell Biol* 33:1183–1192
22. Temple MD, Freebody J, Murray V (2004) Genomic and phylogenetic footprinting at the epsilon-globin silencer region in intact human cells. *Biochim Biophys Acta* 1678:126–134
23. Temple MD, Murray V (2005) Footprinting the ‘essential regulatory region’ of the retinoblastoma gene promoter in intact human cells. *Int J Biochem Cell Biol* 37:665–678
24. Kuo MT, Hsu TC (1978) Bleomycin causes release of nucleosomes from chromatin and chromosomes. *Nature* 271:83–84
25. Galea AM, Murray V (2010) The influence of chromatin structure on DNA damage induced by nitrogen mustards and cisplatin analogues. *Chem Biol Drug Design* 75:578–589
26. Bentley DR, Balasubramanian S, Swerdlow HP, Smith GP, Milton J, Brown CG, Hall KP, Evers DJ, Barnes CL, Bignell HR, Boultell JM, Bryant J et al (2008) Accurate whole human genome sequencing using reversible terminator chemistry. *Nature* 456:53–59
27. Mardis ER (2008) Next-generation DNA sequencing methods. *Annu Rev Genomics Hum Genet* 9:387–402
28. Ma QC, Ennis CA, Aparicio S (2012) Opening Pandora’s box—the new biology of driver mutations and clonal evolution in cancer as revealed by next generation sequencing. *Curr Opin Genet Dev* 22:3–9
29. Boyle AP, Davis S, Shulha HP, Meltzer P, Margulies EH, Weng Z, Furey TS, Crawford GE (2008) High-resolution mapping and characterization of open chromatin across the genome. *Cell* 132:311–322
30. Crawford GE, Holt IE, Whittle J, Webb BD, Tai D, Davis S, Margulies EH, Chen Y, Bernat JA, Ginsburg D, Zhou D, Luo S et al (2006) Genome-wide mapping of DNase hypersensitive sites using massively parallel signature sequencing (MPSS). *Genome Res* 16:123–131
31. Kim TH, Barrera LO, Zheng M, Qu C, Singer MA, Richmond TA, Wu Y, Green RD, Ren B (2005) A high-resolution map of active promoters in the human genome. *Nature* 436:876–880
32. Jiang C, Pugh BF (2009) A compiled and systematic reference map of nucleosome positions across the *Saccharomyces cerevisiae* genome. *Genome Biol* 10:R109
33. Jiang C, Pugh BF (2009) Nucleosome positioning and gene regulation: advances through genomics. *Nat Rev Genet* 10:161–172
34. Schones DE, Cui K, Cuddapah S, Roh TY, Barski A, Wang Z, Wei G, Zhao K (2008) Dynamic regulation of nucleosome positioning in the human genome. *Cell* 132:887–898
35. Wang Z, Schones DE, Zhao K (2009) Characterization of human epigenomes. *Curr Opin Genet Dev* 19:127–134
36. Zhang X, Robertson G, Woo S, Hoffman BG, Gottardo R (2012) Probabilistic inference for nucleosome positioning with MNase-based or sonicated short-read data. *PLoS One* 7:e32095
37. Wei G, Hu G, Cui K, Zhao K (2012) Genome-wide mapping of nucleosome occupancy, histone modifications, and gene expression using next-generation sequencing technology. *Methods Enzymol* 513:297–313
38. Jin B, Ernst J, Tiedemann RL, Xu H, Sureshchandra S, Kellis M, Dalton S, Liu C, Choi JH, Robertson KD (2012) Linking DNA methyltransferases to epigenetic marks and nucleosome structure genome-wide in human tumor cells. *Cell Rep* 2:1411–1424
39. Yigit E, Zhang Q, Xi L, Grilley D, Widom J, Wang JP, Rao A, Pipkin ME (2013) High-resolution nucleosome mapping of targeted regions using BAC-based enrichment. *Nucleic Acids Res* 41:e87
40. Nguyen TV, Chen JK, Murray V (2013) Bleomycin DNA damage: anomalous mobility of 3'-phosphoglycolate termini in an automated capillary DNA sequencer. *J Chromatogr B* 913:113–122
41. Langmead B, Trapnell C, Pop M, Salzberg S (2009) Ultrafast and memory-efficient alignment of short DNA sequences to the human genome. *Genome Biol* 10:R25
42. Li H, Handsaker B, Wysoker A, Fennell T, Ruan J, Homer N, Marth G, Abecasis G, Durbin R (2009) The Sequence Alignment/Map format and SAMtools. *Bioinformatics* 25:2078–2079
43. Kuo MT (1981) Preferential damage of active chromatin by bleomycin. *Cancer Res* 41:2439–2443
44. Reed SD, Fulmer A, Buckholz J, Zhang B, Cutrera J, Shiomiitsu K, Li S (2010) Bleomycin/interleukin-12 electrochemogenetherapy for treating naturally occurring spontaneous neoplasms in dogs. *Cancer Gene Ther* 17:571–578
45. Liu S, Guo Y, Huang R, Li J, Huang S, Kuang Y, Han L, Jiang C (2012) Gene and doxorubicin co-delivery system for targeting therapy of glioma. *Biomaterials* 33:4907–4916
46. Grimwade JE, Cason EB, Beerman TA (1987) Site specificity of bleomycin cleavage in purified and intracellular simian virus 40 DNA. *Nucleic Acids Res* 15:6315–6329

47. Nguyen TV, Murray V (2012) Human telomeric DNA sequences are a major target for the anti-tumour drug, bleomycin. *J Biol Inorgan Chem* 17:1–9
48. Bozeman TC, Nanjunda R, Tang C, Liu Y, Segerman ZJ, Zaleski PA, Wilson WD, Hecht SM (2012) Dynamics of bleomycin interaction with a strongly bound hairpin DNA substrate, and implications for cleavage of the bound DNA. *J Am Chem Soc* 134:17842–17845
49. Giroux RA, Hecht SM (2010) Characterization of bleomycin cleavage sites in strongly bound hairpin DNAs. *J Am Chem Soc* 132:16987–16996
50. Ma Q, Akiyama Y, Xu Z, Konishi K, Hecht SM (2009) Identification and cleavage site analysis of DNA sequences bound strongly by bleomycin. *J Am Chem Soc* 131:2013–2022
51. Ozsolak F, Song JS, Liu XS, Fisher DE (2007) High-throughput mapping of the chromatin structure of human promoters. *Nat Biotechnol* 25:244–248
52. Boeger H, Griesenbeck J, Strattan JS, Kornberg RD (2003) Nucleosomes unfold completely at a transcriptionally active promoter. *Mol Cell* 11:1587–1598
53. Chen K, Xi Y, Pan X, Li Z, Kaestner K, Tyler J, Dent S, He X, Li W (2013) DANPOS: dynamic analysis of nucleosome position and occupancy by sequencing. *Genome Res* 23:341–351